Molecular Genetics and Metabolism Reports 27 (2021) 100767

Contents lists available at ScienceDirect

Molecular Genetics and Metabolism Reports

journal homepage: www.elsevier.com/locate/ymgmr

Reduced macular thickness and macular vessel density in early-treated adult patients with PKU

Csilla Serfozo [a,d], Andras Gellert Barta [b], Endre Horvath [c], Csaba Sumanszki [b], Bela Csakany [a], Miklos Resch [a], Zoltan Zsolt Nagy [a], Peter Reismann [b,*]

[a] Department of Ophthalmology, Faculty of Medicine, Semmelweis University, Maria street 39, 1085 Budapest, Hungary
[b] Department of Internal Medicine and Oncology, Faculty of Medicine, Semmelweis University, Koranyi Sandor street 2/a, 1083 Budapest, Hungary
[c] Independent Statistician, Alsódabas str. 4/2, 1171 Budapest, Hungary
[d] Department of Ophthalmology, Heim Pal Children's Hospital, Ulloi street 86, 1089 Budapest, Hungary

ARTICLE INFO

Keywords:
Dopamine
Macular retinal vessel density
Macular thickness
Optical coherence tomography angiography
Phenylalanine level
Phenylketonuria

ABSTRACT

Purpose: Macular structure is poorly evaluated in early-treated phenylketonuria (ETPKU). To evaluate potential changes, we aimed to examine retinas of PKU patients using optical coherence tomography (OCT) with additional OCT angiography (OCTA) and compare the results to healthy controls.

Methods: A total of 100 adults were recruited in this monocentric, case-control study: 50 patients with ETPKU (mean age: 30.66 ± 8.00 years) and 50 healthy controls (mean age: 30.45 ± 7.18 years). Macular thickness, vessel density and flow area of the right eye was assessed with spectral domain OCT angiography SD-OCT(A). Macular microstructural data between the ETPKU and control group was compared. In the ETPKU group, the relationship between visual functional parameters (best corrected visual acuity [VA], spherical equivalent [SE], contrast sensitivity [CS] and near stereoacuity) and microstructural alterations was examined. The dependency of OCT(A) values on serum phenylalanine (Phe) level was analysed.

Results: There was significant average parafoveal and perifoveal total retinal layer thinning in ETPKU patients compared to healthy controls ($p < 0.016$ and $p < 0.001$, respectively), while the foveal region remained unchanged in the ETPKU group. Whole macular and parafoveal superficial capillary plexus density was significantly decreased in ETPKU compared to controls ($p < 0.001$). There were no significant differences in the foveal avascular zone, nonflow area, macular superficial and deep capillary plexus between the groups. The temporal parafoveal inner retinal layer thickness was found to negatively correlate with individual Phe levels ($r = -0.35$, $p = 0.042$). There was no difference in vascular density and retinal thickness in the subgroup analysis of patients with good therapy adherence compared to patients on a relaxed diet.

Conclusions: Durable elevation in Phe levels are only partially associated with macular retinal structural changes. However, therapy adherence might not influence these ophthalmological complications.

1. Introduction

Phenylketonuria (PKU, OMIM 261600) is a rare, autosomal, recessively inherited disease caused by unfavourable mutations in the phenylalanine hydroxylase gene (PAH). The role of PAH is to convert the essential amino acid Phenylalanine (Phe) into Tyrosine (Tyr) with the

Abbreviations: aminoacid supplements, (AAS); axial length, (AL); contrast sensitivity, (CS); deep capillary plexus, (DCP); diopters, (D); dopamine, (DA); early treated phenylketonuria, (ETPKU); external limiting membrane/inner segment of photoreceptors/outer segment of photoreceptors, (ELM/IS/OS); ganglion cell complex, (GCC); ganglion cell layer, (GCL); inner limiting membrane, (ILM); inner nuclear layer, (INL); inner plexiform layer, (IPL); inner retinal layer, (IRL); intraocular pressure, (IOP); Optical Coherence Tomography, (OCT); Optical Coherence Tomography Angiography, (OCTA); outer nuclear layer, (ONL); outer plexiform layer, (OPL); outer retinal layer, (ORL); Parkinson's disease, (PD); Phenylalanine, (Phe); phenylalanine hydroxylase gene, (PAH); phenylketonuria, (PKU); retinal nerve fiber layer, (RNFL); retinal pigment epithelium, (RPE); signal strength index, (SSI); sine-wave contrast test, (SWCT); spectral domain, (SD); spherical equivalent, (SE); split-spectrum amplitude-decorrelation angiography, (SSADA); superficial capillary plexus, (SCP); tetrahydrobiopterin, (BH4); total retinal layer thickness, (TRLT); Tyrosine, (Tyr); vessel density, (VD); visual acuity, (VA); visual evoked potential, (VEP).

* Corresponding author at: Department of Internal Medicine and Oncology, Semmelweis University, Budapest H-1083, Koranyi Sandor utca 2/a, Hungary.
E-mail address: reismann.peter@med.semmelweis-univ.hu (P. Reismann).

https://doi.org/10.1016/j.ymgmr.2021.100767
Received 7 February 2021; Received in revised form 27 April 2021; Accepted 28 April 2021

cofactor tetrahydrobiopterin (BH4), oxygen and iron [1]. The malfunction of PAH leads to elevated levels of Phe and its metabolites in the blood and brain. Untreated patients present various severe psychiatric and neurologic symptoms including intellectual disability, motor deficits, seizures, and aberrant behaviour [1,2]. PKU was first described by Følling in 1934. Soon thereafter in 1953, the effectiveness of the low-Phe diet was reported to alleviate symptoms in a child with PKU. The approximate incidence of PKU is about 1:10000 in Europe, with significant regional differences [3].

The core elements of preventive therapy are lifelong low-protein diet with the regular consumption of Phe-free amino acid supplements (AAS). In recent years further alternatives have emerged such as BH4 supplementation for responsive patients or glycomacropeptide (GMP), which is an alternative to AAS. Additionally, phenylalanine ammonia-lyase enzyme replacement therapy may also become available to more patients [4].

Since the 1970s, mandatory newborn screening and early initiation of therapy have fundamentally improved quality of life and life expectancy of PKU patients. Those who are diagnosed upon newborn screening and maintain lifelong therapy are called early-treated PKU patients (ETPKU). Most of them lead independent lives and fall within the normal range of general ability [5]. The diagnosis and treatment of PKU is considered to be a medical success, nevertheless social and neuropsychological consequences still occur in some patients [6,7]. Adult patients exhibiting good long-term therapy adherence, and blood Phe levels in the target range (120–600 micromol/l), have significantly higher intellectual abilities compared with suboptimally adherent patients [8].

The precise pathomechanism of neurotoxicity in PKU is unknown. In other neurodegenerative diseases, for instance Parkinson's disease (PD), altered DA metabolism may be one of the possible pathologic mechanisms [9–11]. The widespread modulatory action of dopamine (DA) on visual processing is well known [12]. Some functional ocular deficits found in distinct PD patients [13–17] are likely to be detected in PKU patients as well, such as decreased visual acuity [VA], near stereoacuity, ability to discern colors, contrast sensitivity [CS], and visual evoked potential [VEP] alterations [18–24]. Optical Coherence Tomography (OCT) is of great promise in the evaluation of alterations in PD [25–27]. OCT may provide a new perspective on the visual deficits reported in PKU, and may indirectly provide additional evidence that DA might be the key neurotransmitter in PKU's complications.

Besides neurodegeneration, cerebrovascular [28,29] and retinal microvascular changes have been identified in PD [30,31]. Since the retina is an extension of the central nervous system and its vessels were shown to share many common characteristics with the vasculature of the central nervous system [32], the identification of potential retinal structural changes in PKU might reflect general cerebral alterations affected by the disease [33].

Our group recently described significantly worse functional vision parameters (contrast sensitivity, near stereoacuity, visual acuity) in ETPKU patients compared to healthy controls. Some microstructural changes in the papillary and parapapillary region were also described such as decreased average, superior, inferior GCC thickness, FLV, GLV and average RNFL thickness by OCT [24]. Complementing our previous findings, we report here detailed information on the macular region and microvasculature of ETPKU patients analysed by spectral domain OCT angiography.

2. Patients and methods

2.1. Study design

50 patients (22 female) with ETPKU and 50 healthy controls (22 female) were enrolled in this monocentric, case-control study performed between November 2018 and March 2020. The study adhered to the tenets of the World Medical Association Declaration of Helsinki and relevant national and local requirements, and was approved by the Semmelweis University's Regional, Institutional Scientific and Research Ethics Committee (ETT registration number: SE RKEB 171/2018). All subjects participated voluntarily in the study, individual written informed consent was obtained.

2.2. Study population

2.2.1. PKU patients

Patients who had been diagnosed with PKU during neonatal screening, and had been attending the Inborn Error of Metabolism Adult Metabolic Centre (former 2nd Department of Medicine, Semmelweis University, Budapest) for at least 10 years were enrolled in this study. Inclusion criteria were the following: a.) classical or mild/moderate PKU diagnosed at the time of birth; b.) continuous treatment with dietary protein restriction and amino acid supplements alone; c.) older than 18 years of age; d.) Caucasian origin; e.) good compliance in terms of regular, yearly check-ups at the adult metabolic centre; f.) no history of other systemic or ocular diseases. Exclusion criteria included refractive error over ±5.5 diopters (D) of spherical equivalent refraction or over ±3.0 D of astigmatism, previous ocular trauma or operation. For precise classification of patient phenotypes a combination of methods was used: patients with Phe levels over 1200 μmol/l before therapy initiation were classified as classical PKU, with pretreatment Phe levels of 900–1200 μmol/l as moderate PKU, and pretreatment Phe levels of 600–900 μmol/l as mild PKU. In cases where blood Phe level was not unambiguous - because of early therapy intitiation - course of the disease and phenylalanine tolerance were also assessed [34]. Patients were classified into two groups; (1.) good or (2.) suboptimal diet adherence, in accordance with European guidelines, as detailed elsewhere [24].

2.2.2. Case-matched controls

Controls were case-matched to the ETPKU patient group with respect to age, spherical equivalent (SE), axial length (AL), ethnicity and sex, all known parameters affecting OCT results [35–41]. Inclusion criteria for controls were the following: a.) Caucasian origin; b.) no history of systemic or ocular diseases; c.) age older than 18 years.

2.3. Laboratory tests

Phenylalanine and tyrosine levels were measured by API2000 LC/MS/MS (Perkin-Elmer Sciex, Ontario, Canada) at the 1st Department of Pediatrics, Semmelweis University, Budapest from antecubital blood samples under standardized circumstances in compliance with the recommendations of the European guideline for adult patients with PKU. The analytical methods have been previously described [42].

2.4. Ophthalmological examinations

Participants underwent a comprehensive ophthalmological examination at the Department of Ophthalmology, Semmelweis University, including VA using the Early Treatment Diabetic Retinopathy Study (ETDRS) (2000 series revised) letter visual acuity chart with testing exam at 4 m, which was recorded as the Logarithm of the Minimum Angle of Resolution (LogMAR). A LogMar value of zero indicates good vision, in this case VA is equal to the reference standard (20/20, 1.0), while higher LogMAR values indicate poorer vision. Negative LogMar values indicate better VA than the reference standard. When necessary, VA was assessed with the best spectacle correction. The analysis was based on spherical equivalent, which is the algebraic sum of the value of the sphere and half the cylindrical value. We performed non-contact intraocular pressure (IOP) measurement, anterior and posterior segment examinations using slit lamp biomicroscopy with pupil dilatation and OCT imaging.

2.4.1. Refraction assessment

The refractive assessment was based on objective non-cycloplegic refraction with conventional autorefractor (Accuref-K 9001, Shin Nippon, Japan).

2.4.2. Contrast sensitivity

VA is a quantitative measurement and provides limited information about functional vision [43]. VA quantifies the eye's spatial resolution for highly contrasting objects, whereas CS shows the minimum luminosity difference between these objects. CS measurements were conducted using sine-wave contrast test (SWCT, Arthur P. Ginsburg, Stereo Optical Co.). We excluded participants with strange crossing of the right- and left-sided measured curves or unusual deviation of the curves at the highest spatial frequency. Average CS values were converted to logarithmic form [44–46].

2.4.3. Stereoacuity

We performed near stereoacuity using the Titmus Wirt circles stereotest (Stereo Optical Co., Inc. Chicago, IL) at a distance of 40 cm. Cross polarized filters were used with the participants own near correction in place, if needed. Seconds of arc were transformed to logarithmic units for analysis. Participants with a score of zero circles were excluded because this method is not able to give a precise estimate in such cases [47–49].

2.4.4. Axial length

Average AL was calculated based on five consecutive biometric measurements using Zeiss IOL Master (Carl Zeiss, Germany Version 5.4.4.0006) device which grants high accuracy and reproducibility [50,51].

2.4.5. Intraocular Pressure

Average IOP was calculated by non-contact Tonometer (Topcon CT-1P) with auto alignment and shot function, based on three consecutive measurements [52].

2.4.6. Spectral domain optical coherence tomography

An ultrahigh resolution spectral domain OCT (SD-OCT) system AngioVue™ (RTVue-XR Avanti; Optovue Inc., Fremont, CA, USA, software version 2018.0.0.18) was used to detect retinal parameters [53–55]. This device can in vivo quantitatively measure the morphology of gross retinal histology. Each scan was carried out on the same device to prevent intermachine variability [56]. Scans were automatically segmented by the software and measurements were performed by a single, well-trained examiner on the same day.

2.4.6.1. Retinal layer thickness analysis. Retinal thickness was examined in nine OCT zones of 6x6mm en face images. The central/foveal region was defined as being centered at the fovea in a 1000 μm circle, surrounded by parafoveal (1000 μm to 3000 μm) and perifoveal (3000 μm to 6000 μm) concentric regions. The latter two regions were both subdivided to superior, inferior, temporal, and nasal zones. Total retinal layer thickness (TRLT) is defined from the inner limiting membrane (ILM) to the retinal pigment epithelium (RPE). The inner retinal layer (IRL) is located between the ILM and the outer boundary of the inner plexiform layer (IPL). IRL consists of RNFL, ganglion cell layer (GCL) and IPL. The outer retinal layer (ORL) is defined between the outer boundary of IPL and the outer edges of RPE. It contains the inner nuclear layer (INL), outer plexiform layer (OPL), outer nuclear layer (ONL), external limiting membrane/inner segment of photoreceptors/outer segment of photoreceptors (ELM/IS/OS), and the RPE. The foveal TRL thickness is equal to the ORL thickness, because no inner layers exist in the foveal center (Picture 1).

2.4.6.2. Vessel density analysis. Optical Coherence Tomography Angiography (OCTA) provides in vivo non-invasive volumetric angiography images without the need to inject any extrinsic dye contrast. This novel technology allows quantification of the vessel density (VD) around the macula, defined as the percentage of the area occupied by vessels. We evaluated the superficial capillary plexus (SCP) and the deep capillary plexus (DCP) in the macular region of the 3 × 3 angio cube scan (3x3mm area centered on the fovea) with the split-spectrum amplitude-decorrelation angiography (SSADA) algorithm. SCP was obtained between the ILM and the inner boundary of IPL. DCP was examined between the outer boundary of IPL and the outer boundary of OPL of the retina. The en face images of SCP and DCP were segmented using the AngioAnalytics software. In the SCP, the nonflow area (mm^2) within the foveal avascular zone (FAZ) and the FAZ area (mm^2) were measured by differentiating the boundaries of the nonflow and flow areas using the OCTA intrinsic software.

The vessels in the RNFL, GCL and superficial IPL are defined as SCP. Deeper IPL, INL and OPL receive blood from the DCP [57,58].

Only good-quality images were included. Results were excluded from further analyses in the following cases: low signal strength or local weak signal (retina map SSI under 60%, angio retina scan quality under 7), image cropping, poor fixation leading to motion, blinking or doubling artifacts [59].

2.5. Statistical analysis

Statistical analyses were carried out using the software SPSS Statistics for Windows, version 17.0 (SPSS Inc., Chicago, Ill., USA). The Shapiro-Wilk test was used for normality testing due to small sample size. For normally distributed variables parametric tests were used, and for non-normally distributed variables we used non-parametric tests. Means were compared between groups using Mann-Whitney *U* test and one-way ANOVA. Continuous data are reported as mean and standard deviation. Categorical data were tested with Chi-square. Continuous

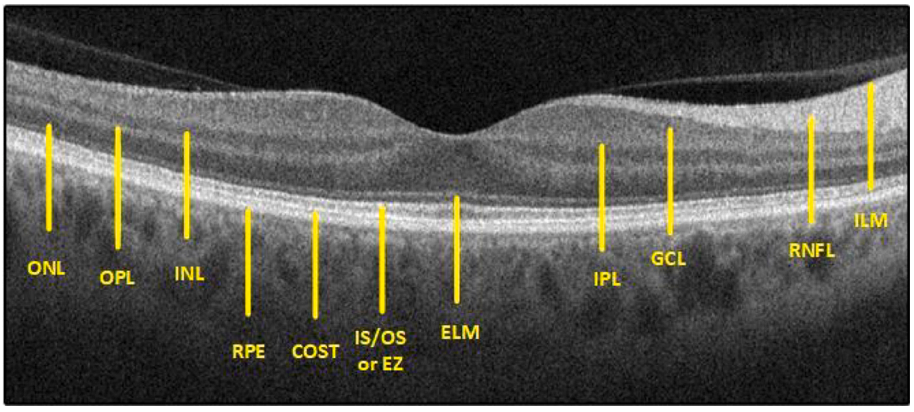

Picture 1. Normal retinal layers in a SD-OCT scan. COST: cones outer segment tips line; ELM: external limiting membrane; GCL: ganglion cell layer; ILM: inner limiting membrane; IS/OS or EZ: inner segment outer segment junction line or ellipsoid zone, INL: inner nuclear layer; IPL: inner plexiform layer; ONL: outer nuclear layer; OPL: outer plexiform layer; RNFL: retinal nerve fiber layer; RPE: retinal pigmented epithelium.

variables were analysed with Kendall's Tau-b correlation. Multiple linear regression was executed where possible. A p-value of <0.05 was considered statistically significant.

3. Results

In the ETPKU group, the mean age was 30.66 ± 8.00 years. Mean Phe level over the last ten years was slightly higher than the upper target level for adult PKU patients (618 ± 217 μmol/L) whereas mean Phe/Tyr ratio was 16.9 ± 8.

The mean age was 30.45 ± 7.18 years in case-matched controls, Phe level was not measured. There were no significant differences in age, SE, IOP, AL or sex between the groups (Table 1). SE was between +1.8 and −5.5 D in the ETPKU and between +1.37 and −4.5 D in the control group (Table 1).

3.1. Retinal thickness of patients with ETPKU versus controls

Mean foveal thickness in the 1 mm zone was 252.97 ± 22.14 μm in the ETPKU group and 251.47 ± 17.99 μm in the control group (p = 0.73). The parafoveal (303.25 ± 15.44 μm vs 311.39 ± 14.91 μm, p = 0.016) and perifoveal TRLT (275.33 ± 12.55 μm vs 284.65 ± 13.06 μm [p = 0.001]) were significantly lower in the ETPKU group than in the control group. Patients with ETPKU had significantly decreased TRLT in temporal and superior parafoveal zones and in all regions of the perifoveal zone (temporal, superior, nasal, inferior) when compared to controls (Table 2). Similar differences were found in IRL thickness in the para- and perifoveal zone in all regions (Table 3).

With the exception of the perifoveal temporal zone there were no significant differences in ORL thickness between the groups in the para- or perifoveal area (Table 4).

In the ETPKU group, ganglion cell complex (GCC) thickness showed significant correlation with parafoveal and perifoveal TRLT and with VD parameters of the macula (Table 5).

3.2. Macular microvasculature in patients with ETPKU vs controls

The retinal nonflow area (ETPKU: 0.43 ± 0.15 mm^2 vs controls: 0.45 ± 0.9 mm^2, p = 0.42) and the superficial FAZ (ETPKU: 0.26 ± 0.14 mm^2 vs controls:0.25 ± 0.09 mm^2, p = 0.58) were similar in the two groups. Significantly decreased VD was seen in the whole macular and parafoveal region of patients with PKU, detailed parameters are presented in Table 6.

3.3. Metabolic and ophthalmological parameters in the ETPKU group

We examined the potential link between diet adherence based on individual Phe levels in the last 10 years (good [n = 24] and suboptimal [n = 26] diet adherence groups), retinal thickness and vascular density parameters. Only temporal parafoveal IRL thickness correlated with individual Phe levels (r = −0.35, p = 0.042; Pearson correlation). Neither retinal thickness nor vascular density correlated with functional parameters (VA, CS, strereoacuity).

Table 1
Comparison of demographic data and structural biometric characteristics between patients with ETPKU and healthy controls at baseline. We used one-way ANOVA for age, SE, IOP and AL, and Chi-square test for the sex comparison. Significance: $p < 0.05$. AL: axial length, IOP: intraocular pressure, SD: standard deviation, SE: spherical equivalent, VA: visual acuity.

Characteristic, mean ± SD	ETPKU (n = 50)	Control (n = 50)	p-value
Age (years)	30.66 ± 8.00	30.44 ± 7.18	0.890
Sex, n (%)			
Female	28 (56%)	28 (56%)	0.999
Male	22 (44%)	22 (44%)	0.999
SE (dioptre)	−0.72 ± 1.22	−0.42 ± 1.01	0.173
IOP (mmHg)	17.15 ± 2.15	17.26 ± 2.19	0.795
AL (mm)	23.37 ± 0.81	23.44 ± 0.62	0.625
VA (logMAR)	−0.016 ± 0.18	−0.16 ± 0.06	**<0.001**

Table 2
Group comparison of total retinal thickness between patients with ETPKU and controls. Mean and SD values are given in μm. One-way ANOVA was used to compare mean differences. ETPKU: Early treated phenylketonuria, inf.: inferior, nas.: nasal, sup.: superior, temp.: temporal.

Characteristic, mean ± SD		ETPKU	CONTROL	P
PARA-FOVEAL	temp.	294.36 ± 14.81	303.18 ± 14.81	**0.008**
	sup.	304.81 ± 15.56	315.41 ± 15.93	**0.003**
	nas.	309.17 ± 17.72	315.49 ± 15.46	0.084
	inf.	305.06 ± 15.86	311.37 ± 13.48	0.051
PERI-FOVEAL	temp.	264.03 ± 12.17	274.24 ± 13.14	**<0.001**
	sup	277.78 ± 13.32	286.96 ± 14.17	**0.003**
	nas.	287.53 ± 24.74	298.71 ± 21.29	**0.028**
	inf.	268.89 ± 12.69	277.76 ± 12.65	**0.002**

Bold indicates significant difference (p<0.05).

Table 3
Group comparison of inner retinal thickness between patients with ETPKU and controls. Mean and SD values are given in μm. One-way ANOVA was used to compare mean differences. ETPKU: Early treated phenylketonuria, inf.: inferior, nas.: nasal, sup.: superior, temp.: temporal.

Characteristic, mean ± SD		ETPKU	CONTROL	P
PARA-FOVEAL	temp.	118.12 ± 9.06	122.67 ± 8.92	**0.027**
	sup.	124.41 ± 9.05	134.65 ± 9.21	**<0.001**
	nas.	123.18 ± 12.25	133.94 ± 10.07	**<0.001**
	inf.	126.94 ± 9.74	132.56 ± 10.54	**0.016**
PERI-FOVEAL	temp.	103.79 ± 7.07	107.98 ± 6.79	**0.008**
	sup	107.97 ± 5.64	113.81 ± 6.19	**<0.001**
	nas.	115.56 ± 7.74	125.04 ± 8.64	**<0.001**
	inf.	106.65 ± 6.47	112.13 ± 6.67	**<0.001**

Bold indicates significant difference (p<0.05).

Table 4
Group comparison of outer retinal thickness between patients with ETPKU and controls. Mean and SD are given in μm. One-way ANOVA was used to compare mean differences. ETPKU: Early treated phenylketonuria, inf.: inferior, nas.: nasal, sup.: superior, temp.: temporal.

Characteristic, mean ± SD		ETPKU	CONTROL	P
PARA-FOVEAL	temp.	175.53 ± 11.85	180.40 ± 10.26	0.051
	sup.	179.41 ± 10.75	177.60 ± 26.42	0.707
	nas.	184.74 ± 12.95	181.75 ± 8.61	0.213
	inf.	177.09 ± 10.90	177.31 ± 7.52	0.912
PERI-FOVEAL	temp.	160.00 ± 12.27	166.23 ± 8.82	**0.003**
	sup	169.47 ± 10.11	172.75 ± 9.81	0.145
	nas.	174.26 ± 11.45	175.52 ± 8.81	0.576
	inf.	162.15 ± 8.58	165.35 ± 7.40	0.074

Bold indicates significant difference (p<0.05).

4. Discussion

ETPKU patients - owing to the neonatal screening and early-introduced, life-long Phe-lowering therapy - are protected from the most severe consequences of the disease. Although the impact of ETPKU on the eye has not been substantially examined yet, earlier studies showed, that untreated PKU may cause various ocular deficits in some patients, but thorough exmination of the retina was not available at that time [22,23,60]. Therefore, we aimed to investigate the presence and potential correlation between predicted functional ophthalmological alterations (visual acuity, contrast sensitivity, near stereoacuity) and retinal changes (thickness of inner and outer macular retinal layers and macular microvasculature measured by SD-OCT(A) with automatic segmentation techniques) in ETPKU patients with OCT. This is a

Table 5
Correlation analysis between macular TRLT and VD values with GCC values in the ETPKU group. Kendall's T Correlation (2 tailed) was used to measure the association between variables. TRLT and GCC are given in μm. ave.: average, ETPKU: Early treated phenylketonuria, GCC: ganglion cell layer, inf.: inferior, sup.: superior, TRLT: total retinal layer thickness, VD: vessel density.

		Parafoveal TRLT	Perifoveal TRLT	Macular superficial VD whole image (%)	Superficial VD parafovea (%)
GCC average	Correlation Coefficient	0.31	0.37	0.37	0.38
	p-value	**0.021**	**0.005**	**0.001**	**0.001**
GCC superior	Correlation Coefficient	0.31	0.42	0.32	0.32
	p-value	**0.021**	**0.002**	**0.005**	**0.004**
GCC inferior	Correlation Coefficient	0.30	0.39	0.34	0.36
	p-value	**0.022**	**0.003**	**0.003**	**0.002**

Bold indicates significant difference ($p<0.05$).

Table 6
Group comparison of vascular density between patients with ETPKU and controls. One-way ANOVA was used to compare mean differences. ETPKU: Early treated phenylketonuria, sup.: superficial.

Characteristic, mean ± SD	ETPKU	CONTROL	p-value
Macular sup. density whole image (%)	46.62 ± 2.41	48.40 ± 2.12	**<0.001**
Sup. density fovea (%)	20.81 ± 8.05	19.17 ± 4.90	0.223
Sup. density parafovea (%)	48.93 ± 2.87	51.27 ± 2.33	**<0.001**
Macular deep density whole image (%)	54.72 ± 3.10	54.49 ± 2.58	0.707
Deep density fovea (%)	35.07 ± 8.96	36.35 ± 6.42	0.429
Deep density parafovea (%)	57.19 ± 2.41	56.65 ± 2.24	0.271

Bold indicates significant difference ($p<0.05$).

consecutive report of our investigations in a relatively large PKU adult population [24].

The macular vascular region has not been previously evaluated in ETPKU, and there has been also very limited data available regarding the standard OCT-structure of these patients. In the single report available in the English literature by Hopf et al. [20], the authors did not describe retinal alterations of 19 ETPKU patients compared to non-matched controls. In contrast to this, our examination here in a larger, case-controlled setting revealed marked thinning in the para- and perifoveal retinal regions. CT is the most precise technique to measure retinal thickness and has excellent repeatability. Upon analysing the scans we found significant IRL thinning in the para- and perifoveal region of patients with ETPKU when compared to healthy controls. In our previous study [24], we reported that the mean ganglion cell complex (GCC) thickness values (GCL + IPL + RNFL) were significantly decreased in patients with ETPKU when compared to healthy individuals.

The pathophysiology of the observed alterations, and whether VD alterations are primary or secondary consequences of PKU are not known. This study was not designed to evaluate the background of the found differences, but to raise awareness of the ophthalmological consequences for future research. One might think, that alterations in neurotransmitter availability, particularly in DA levels may have an impact on these findings in PKU. DA has a complex role in visual processing as a neurotransmitter and as a modulator in vision. DA-containing neurons are the amacrine cells and the interplexiform cells, which are located in the INL and IPL, respectively [61,62].

IRL thinning with potential dopaminergic neurodegeneration in the background has been reported in various diseases such as multiple sclerosis, Alzheimer's disease, preperimetric glaucoma, and also in PD [63–66]. The exact pathomechanism in PKU is not clear yet. We hypothesize that primary degeneration, secondary loss of retinal dopamine-regulated neurons or secondary transsynaptic neuronal damage may cause the discussed conditions. Dopaminergic cells are located mainly in the INL, and account for fewer than 10% of the INL's cell bodies, therefore modified dopaminergic actions can be only one of many factors that could explain the measured retinal alterations. [61,67,68]. As a next step, dopamine action should be investigated in these affected layers.

Despite marked changes in most areas, not all of the retinal regions showed thinning. ORLT seemed to be relatively unaffected, except for a single segment. Similar results were documented in other diseases, such as in PD by some [69,70], but not all author [68,71]. In terms of retinal vasculature, we found decreased microvascular density only in the superficial layer, but not in deep layers of ETPKU patients. Similar findings were reported in glaucomatous eyes [72,73]. The significance of this observation should be further evaluated in future projects, our research is the first to provide data in PKU.

We did not find correlation between disease severity or duration and GCC-IPL layer thickness, which is a similar result to other reports about neurodegenerative diseases affecting dopaminergic cells, such as PD [74,75]. The lack of observed correlation with disease severity or metabolic control may suggest that these impairments appear early in life, or could reflect a high degree of sensitivity of these cell layers.

It is important to note that this study has some limitations. In order to distinguish the alteration of the dopaminergic amacrine cell body layer, further segmentation of the INL should be performed. The fact that no currently available device can analyse the amacrine, bipolar, Müller, horizontal cells, interplexiform neurons and displaced ganglion cells separately in vivo, is a limiting factor. In contrast, retinal microvasculature could be better assessed in the middle capillary plexus technically, but this is generally not supported in current OCTA softwares.

5. Conclusion

Untreated PKU can cause severe ocular deficits. Various studies suggest an involvement of the retina in neurodegenerative diseases, such as PD. Although PKU is an inborn metabolic disease, some similarity can be found in the retinal alterations with aforementioned neurodegenerative diseases. We conclude, that PKU in early-treated adults is associated with decreased microvascular density in the superficial layer and thinning is detectable in TRLT in the temporal and superior parafoveal zones, in all regions of the perifoveal zone, in IRL thickness in the para- and perifoveal and in ORL thickness in the perifoveal temporal areas. Our findings suggest that further studies are necessary to evaluate these results and to clarify the underlying pathophysiological factors.

Contributors

CsSe, ZZsN and PR: conceptualization, planning and methodology of study. CsSe: patient examination and data aquisition. CsSe, AGB, CsSu, ZZsN and PR: data curation and validation. CsSe, AGB and EH: formal statistical analysis. CsSe, BCs, MR, ZZsN: data interpretation. CsSe: writing - original draft. CsSe, CsSu, AGB and PR: review & editing.

Ethics approval

The study followed the principles of the guidelines in the World Medical Association Declaration of Helsinki of 1975 and was approved by the Semmelweis University's Regional, Institutional Scientific and Research Ethics Committee (ETT registration number: SE RKEB 171/2018).

Conflict of interest statement

The authors have no conflict of interest to report.

Financial disclosures

There are no financial conflicts of interest to disclose.

References

[1] N. Blau, F.J. van Spronsen, H.L. Levy, Phenylketonuria, Lancet 376 (9750) (2010) 1417–1427.
[2] S.E. Waisbren, et al., Phenylalanine blood levels and clinical outcomes in phenylketonuria: a systematic literature review and meta-analysis, Mol. Genet. Metab. 92 (1–2) (2007) 63–70.
[3] J.G. Loeber, Neonatal screening in Europe; the situation in 2004, J. Inherit. Metab. Dis. 30 (4) (2007) 430–438.
[4] A.M.J. van Wegberg, et al., The complete European guidelines on phenylketonuria: diagnosis and treatment, Orphanet J. Rare Dis. 12 (1) (2017) 162.
[5] J. Vockley, et al., Phenylalanine hydroxylase deficiency: diagnosis and management guideline, Genet. Med. 16 (2) (2014) 188–200.
[6] J.J. Moyle, et al., Meta-analysis of neuropsychological symptoms of adolescents and adults with PKU, Neuropsychol. Rev. 17 (2) (2007) 91–101.
[7] A.E. ten Hoedt, et al., High phenylalanine levels directly affect mood and sustained attention in adults with phenylketonuria: a randomised, double-blind, placebo-controlled, crossover trial, J. Inherit. Metab. Dis. 34 (1) (2011) 165–171.
[8] R. Koch, et al., Phenylketonuria in adulthood: a collaborative study, J. Inherit. Metab. Dis. 25 (5) (2002) 333–346.
[9] M.B. Djamgoz, et al., Neurobiology of retinal dopamine in relation to degenerative states of the tissue, Vis. Res. 37 (24) (1997) 3509–3529.
[10] C. Harnois, T. Di Paolo, Decreased dopamine in the retinas of patients with Parkinson's disease, Invest. Ophthalmol. Vis. Sci. 31 (11) (1990) 2473–2475.
[11] H. Ikeda, G.M. Head, C.J. Ellis, Electrophysiological signs of retinal dopamine deficiency in recently diagnosed Parkinson's disease and a follow up study, Vis. Res. 34 (19) (1994) 2629–2638.
[12] R. Brandies, S. Yehuda, The possible role of retinal dopaminergic system in visual performance, Neurosci. Biobehav. Rev. 32 (4) (2008) 611–656.
[13] R.D. Jones, I.M. Donaldson, P.L. Timmings, Impairment of high-contrast visual acuity in Parkinson's disease, Mov. Disord. 7 (3) (1992) 232–238.
[14] J.T. Hutton, et al., Spatial contrast sensitivity is reduced in bilateral Parkinson's disease, Neurology 41 (8) (1991) 1200–1202.
[15] I. Bodis-Wollner, Visual electrophysiology in Parkinson's disease: PERG, VEP and visual P300, Clin. Electroencephalogr. 28 (3) (1997) 143–147.
[16] D. Regan, D. Neima, Low-contrast letter charts in early diabetic retinopathy, ocular hypertension, glaucoma, and Parkinson's disease, Br. J. Ophthalmol. 68 (12) (1984) 885–889.
[17] M.J. Price, et al., Abnormalities in color vision and contrast sensitivity in Parkinson's disease, Neurology 42 (4) (1992) 887–890.
[18] A. Diamond, C. Herzberg, Impaired sensitivity to visual contrast in children treated early and continuously for phenylketonuria, Brain 119 (Pt 2) (1996) 523–538.
[19] G. Gramer, et al., Visual functions in phenylketonuria-evaluating the dopamine and long-chain polyunsaturated fatty acids depletion hypotheses, Mol. Genet. Metab. 108 (1) (2013) 1–7.
[20] S. Hopf, et al., Saccadic reaction time and ocular findings in phenylketonuria, Orphanet J. Rare Dis. 15 (1) (2020) 124.
[21] S.J. Jones, et al., Visual evoked potentials in phenylketonuria: association with brain MRI, dietary state, and IQ, J. Neurol. Neurosurg. Psychiatry 59 (3) (1995) 260–265.
[22] R. Korinthenberg, K. Ullrich, F. Füllenkemper, Evoked potentials and electroencephalography in adolescents with phenylketonuria, Neuropediatrics 19 (4) (1988) 175–178.
[23] J. Zwaan, Eye findings in patients with phenylketonuria, Arch. Ophthalmol. 101 (8) (1983) 1236–1237.
[24] C. Serfozo, et al., Altered visual functions, macular ganglion cell and papillary retinal nerve fiber layer thickness in early-treated adult PKU patients, Mol. Genet. Metab. Rep. 25 (2020) 100649.
[25] C.R. Adam, et al., Correlation of inner retinal thickness evaluated by spectral-domain optical coherence tomography and contrast sensitivity in Parkinson disease, J. Neuroophthalmol. 33 (2) (2013) 137–142.
[26] T.S. Aydin, et al., Optical coherence tomography findings in Parkinson's disease, Kaohsiung J. Med. Sci. 34 (3) (2018) 166–171.
[27] M. Unlu, et al., Correlations among multifocal electroretinography and optical coherence tomography findings in patients with Parkinson's disease, Neurol. Sci. 39 (3) (2018) 533–541.
[28] R.S. Schwartz, et al., Small-vessel disease in patients with Parkinson's disease: a clinicopathological study, Mov. Disord. 27 (12) (2012) 1506–1512.
[29] J. Guan, et al., Vascular degeneration in Parkinson's disease, Brain Pathol. 23 (2) (2013) 154–164.
[30] W.R. Kwapong, et al., Retinal microvascular impairment in the early stages of Parkinson's disease, Invest. Ophthalmol. Vis. Sci. 59 (10) (2018) 4115–4122.
[31] R. Kromer, et al., Evaluation of retinal vessel morphology in patients with Parkinson's disease using optical coherence tomography, PLoS One 11 (8) (2016), e0161136.
[32] A. London, I. Benhar, M. Schwartz, The retina as a window to the brain-from eye research to CNS disorders, Nat. Rev. Neurol. 9 (1) (2013) 44–53.
[33] I.J. MacCormick, G. Czanner, B. Faragher, Developing retinal biomarkers of neurological disease: an analytical perspective, Biomark. Med 9 (7) (2015) 691–701.
[34] P. Guldberg, et al., A European multicenter study of phenylalanine hydroxylase deficiency: classification of 105 mutations and a general system for genotype-based prediction of metabolic phenotype, Am. J. Hum. Genet. 63 (1) (1998) 71–79.
[35] F. Gómez-Ulla, et al., Age and gender influence on foveal avascular zone in healthy eyes, Exp. Eye Res. 189 (2019) 107856.
[36] A. Takeyama, et al., Influence of axial length on ganglion cell complex (GCC) thickness and on GCC thickness to retinal thickness ratios in young adults, Jpn. J. Ophthalmol. 58 (1) (2014) 86–93.
[37] W.K. Song, et al., Macular thickness variations with sex, age, and axial length in healthy subjects: a spectral domain-optical coherence tomography study, Invest. Ophthalmol. Vis. Sci. 51 (8) (2010) 3913–3918.
[38] B. Kremser, et al., Retinal thickness analysis in subjects with different refractive conditions, Ophthalmologica 213 (6) (1999) 376–379.
[39] L.Y. Chun, et al., Differences in macular capillary parameters between healthy black and white subjects with Optical Coherence Tomography Angiography (OCTA), PLoS One 14 (10) (2019), e0223142.
[40] N.A. Iafe, et al., Retinal capillary density and Foveal avascular zone area are age-dependent: quantitative analysis using optical coherence tomography angiography, Invest. Ophthalmol. Vis. Sci. 57 (13) (2016) 5780–5787.
[41] S. Ooto, M. Hangai, N. Yoshimura, Effects of sex and age on the normal retinal and choroidal structures on optical coherence tomography, Curr. Eye Res. 40 (2) (2015) 213–225.
[42] C. Sumanszki, et al., Metabolic and catecholamine response to sympathetic stimulation in early-treated adult male patients with phenylketonuria, Hormones (Athens) 19 (3) (2020) 395–402.
[43] A. Ginsburg, Contrast sensitivity and functional vision, Int. Ophthalmol. Clin. 43 (2003) 5–15.
[44] L.A. Levin, F.H. Adler, Adler's Physiology of the Eye, Saunders/Elsevier, Edingburg, 2011.
[45] Z. Zalevsky, et al., Thin spectacles for myopia, presbyopia and astigmatism insensitive vision, Opt. Express 15 (17) (2007) 10790–10803.
[46] P.G.J. Barten, Contrast Sensitivity of the Human Eye and its Effects on Image Quality, Technische Universiteit Eindhoven, Eindhoven, 1999, p. 88.
[47] K.R. Sitko, et al., Pitfalls in the use of stereoacuity in the diagnosis of nonorganic visual loss, Ophthalmology 123 (1) (2016) 198–202.
[48] T.R. Fricke, J. Siderov, Stereopsis, stereotests, and their relation to vision screening and clinical practice, Clin. Exp. Optom. 80 (5) (1997) 165–172.
[49] B. Antona, et al., Intraexaminer repeatability and agreement in stereoacuity measurements made in young adults, Int. J. Ophthalmol. 8 (2) (2015) 374–381.
[50] R. Connors 3rd, P. Boseman 3rd, R.J. Olson, Accuracy and reproducibility of biometry using partial coherence interferometry, J Cataract Refract Surg 28 (2) (2002) 235–238.
[51] H. Eleftheriadis, IOLMaster biometry: refractive results of 100 consecutive cases, Br. J. Ophthalmol. 87 (8) (2003) 960–963.
[52] S.P. Bang, C.E. Lee, Y.C. Kim, Comparison of intraocular pressure as measured by three different non-contact tonometers and goldmann applanation tonometer for non-glaucomatous subjects, BMC Ophthalmol. 17 (1) (2017) 199.
[53] Y. Jia, et al., Quantitative OCT angiography of optic nerve head blood flow, Biomed. Opt. Express 3 (12) (2012) 3127–3137.
[54] S.S. Gao, et al., Optical coherence tomography angiography, Invest. Ophthalmol. Vis. Sci. 57 (9) (2016). Oct27–36.
[55] R.F. Spaide, J.M. Klancnik Jr., M.J. Cooney, Retinal vascular layers imaged by fluorescein angiography and optical coherence tomography angiography, JAMA Ophthalmol. 133 (1) (2015) 45–50.
[56] G.N. Magrath, et al., Variability in foveal avascular zone and capillary density using optical coherence tomography angiography machines in healthy eyes, Retina 37 (11) (2017) 2102–2111.
[57] J.P. Campbell, et al., Detailed vascular anatomy of the human retina by projection-resolved optical coherence tomography angiography, Sci. Rep. 7 (2017) 42201.
[58] R.F. Spaide, C.A. Curcio, Evaluation of segmentation of the superficial and deep vascular layers of the retina by optical coherence tomography angiography instruments in Normal eyes, JAMA Ophthalmol. 135 (3) (2017) 259–262.
[59] G.E. Lang, et al., Accurate OCT-angiography interpretation - detection and exclusion of artifacts, Klin. Monatsbl. Augenheilkd. 234 (9) (2017) 1109–1118.
[60] L. Cotticelli, et al., Ophthalmological findings of phenylketonuria: a survey of 14 cases, J. Pediatr. Ophthalmol. Strabismus 22 (2) (1985) 78–79.
[61] J.M. Frederick, et al., Dopaminergic neurons in the human retina, J. Comp. Neurol. 210 (1) (1982) 65–79.
[62] M. Schütte, P. Witkovsky, Dopaminergic interplexiform cells and centrifugal fibres in the Xenopus retina, J. Neurocytol. 20 (3) (1991) 195–207.
[63] A. Cruz-Herranz, et al., Monitoring retinal changes with optical coherence tomography predicts neuronal loss in experimental autoimmune encephalomyelitis, J. Neuroinflammation 16 (1) (2019) 203.
[64] Y. Kotera, et al., Three-dimensional imaging of macular inner structures in glaucoma by using spectral-domain optical coherence tomography, Invest. Ophthalmol. Vis. Sci. 52 (3) (2011) 1412–1421.
[65] P. Zabel, et al., Quantitative Assessment of Retinal Thickness and Vessel Density Using Optical Coherence Tomography Angiography in Patients with Alzheimer's Disease and Glaucoma, 2020. Research Square.
[66] M.E. Hajee, et al., Inner retinal layer thinning in Parkinson disease, Arch. Ophthalmol. 127 (6) (2009) 737–741.

[67] P. Witkovsky, R. Gábriel, D. Krizaj, Anatomical and neurochemical characterization of dopaminergic interplexiform processes in mouse and rat retinas, J. Comp. Neurol. 510 (2) (2008) 158–174.
[68] N.M. Roth, et al., Photoreceptor layer thinning in idiopathic Parkinson's disease, Mov. Disord. 29 (9) (2014) 1163–1170.
[69] A. Uchida, et al., Outer retinal assessment using spectral-domain optical coherence tomography in patients with Alzheimer's and Parkinson's disease, Invest. Ophthalmol. Vis. Sci. 59 (7) (2018) 2768–2777.
[70] M.E. Hajee, et al., Inner retinal layer thinning in Parkinson disease, Arch. Ophthalmol. 127 (6) (2009) 737–741.
[71] P. Mailankody, et al., Optical coherence tomography as a tool to evaluate retinal changes in Parkinson's disease, Parkinsonism Relat. Disord. 21 (10) (2015) 1164–1169.
[72] H.S. Chen, et al., Optical coherence tomography angiography of the superficial microvasculature in the macular and peripapillary areas in glaucomatous and healthy eyes, Invest. Ophthalmol. Vis. Sci. 58 (9) (2017) 3637–3645.
[73] H.L. Takusagawa, et al., Projection-resolved optical coherence tomography angiography of macular retinal circulation in glaucoma, Ophthalmology 124 (11) (2017) 1589–1599.
[74] M. Kaur, et al., Correlation between structural and functional retinal changes in Parkinson disease, J. Neuroophthalmol. 35 (3) (2015) 254–258.
[75] M. Živković, et al., Retinal ganglion cell/inner plexiform layer thickness in patients with Parkinson's disease, Folia Neuropathol. 55 (2) (2017) 168–173.